ADVANCED MATERIALS
www.advmat.de

Thermosensitive Hydrogel Based on PEO–PPO–PEO Poloxamers for a Controlled In Situ Release of Recombinant Adeno-Associated Viral Vectors for Effective Gene Therapy of Cartilage Defects

*Henning Madry, Liang Gao, Ana Rey-Rico, Jagadeesh K. Venkatesan, Kathrin Müller-Brandt, Xiaoyu Cai, Lars Goebel, Gertrud Schmitt, Susanne Speicher-Mentges, David Zurakowski, Michael D. Menger, Matthias W. Laschke, and Magali Cucchiarini**

Advanced biomaterial-guided delivery of gene vectors is an emerging and highly attractive therapeutic solution for targeted articular cartilage repair, allowing for a controlled and minimally invasive delivery of gene vectors in a spatiotemporally precise manner, reducing intra-articular vector spread and possible loss of the therapeutic gene product. As far as it is known, the very first successful in vivo application of such a biomaterial-guided delivery of a potent gene vector in an orthotopic large animal model of cartilage damage is reported here. In detail, an injectable and thermosensitive hydrogel based on poly(ethylene oxide) (PEO)–poly(propylene oxide) (PPO)–PEO poloxamers, capable of controlled release of a therapeutic recombinant adeno-associated virus (rAAV) vector overexpressing the chondrogenic *sox9* transcription factor in full-thickness chondral defects, is applied in a clinically relevant minipig model in vivo. These comprehensive analyses of the entire osteochondral unit with multiple standardized evaluation methods indicate that rAAV-FLAG-h*sox9*/PEO–PPO–PEO hydrogel-augmented microfracture significantly improves cartilage repair with a collagen fiber orientation more similar to the normal cartilage and protects the subchondral bone plate from early bone loss.

Defects of the articular cartilage, the smooth white tissue covering the ends of bones, do not regenerate and may induce osteoarthritis (OA),[1] the number one cause of chronic disability in the USA, afflicting more than 67 million people by 2030[2] with total treatment costs exceeding $3 billion annually,[3] thus confronting our society with enormous problems. Advanced biomaterial-guided delivery of gene carriers like clinically adapted recombinant adeno-associated virus (rAAV) vectors is an emerging and attractive therapeutic solution for targeted articular cartilage repair, allowing for a controlled and minimally invasive delivery of gene vectors in a spatiotemporally precise manner, reducing intra-articular vector spread and possible loss of the therapeutic gene product.[4]

PEO–PPO–PEO copolymers are nonionic triblock copolymers based on hydrophilic poly(ethylene oxide) (PEO) and hydrophobic poly(propylene oxide) (PPO) (**Figure 1**a)[5] in a linear and bifunctional form (poloxamers) or X-shaped form linked by a dyamine central core (poloxamines) (Figure 1a). These copolymers are self-assembling and temperature sensitive, i.e., at concentrations higher than the critical micellar concentration (CMC), the individual block copolymers (unimers) can self-assemble into micelles. Likewise, by increasing temperature and concentration, the micelles further form 3D networks (gels) with high viscosity,[6] displaying a sol–gel transition around 37 °C, enabling a minimally invasive in vivo injection (an attractive feature for cartilage defects), and becoming semi-solid to solid gels capable of a sustained and controlled release of agents at the place of implantation (Figure 1b).

These micellar systems have the ability to enhance rAAV-based overexpression of reporter[7,8] or chondrogenic genes such as

Prof. H. Madry, Dr. L. Gao, Dr. A. Rey-Rico, Dr. J. K. Venkatesan, Dr. K. Müller-Brandt, Dr. X. Cai, Dr. L. Goebel, G. Schmitt, S. Speicher-Mentges, Prof. M. Cucchiarini
Center of Experimental Orthopaedics
Saarland University Medical Center and Saarland University
D-66421 Homburg, Saarland, Germany
E-mail: magali.madry@uks.eu

The ORCID identification number(s) for the author(s) of this article can be found under https://doi.org/10.1002/adma.201906508.

DOI: 10.1002/adma.201906508

Prof. H. Madry, Dr. L. Goebel
Department of Orthopaedic Surgery
Saarland University Medical Center and Saarland University
D-66421 Homburg, Saarland, Germany

Prof. D. Zurakowski
Department of Anaesthesia
Boston Children's Hospital and Harvard Medical School
Boston, MA 02115, USA

Prof. M. D. Menger, Prof. M. W. Laschke
Institute for Clinical and Experimental Surgery
Saarland University Medical Center and Saarland University
D-66421 Homburg, Saarland, Germany

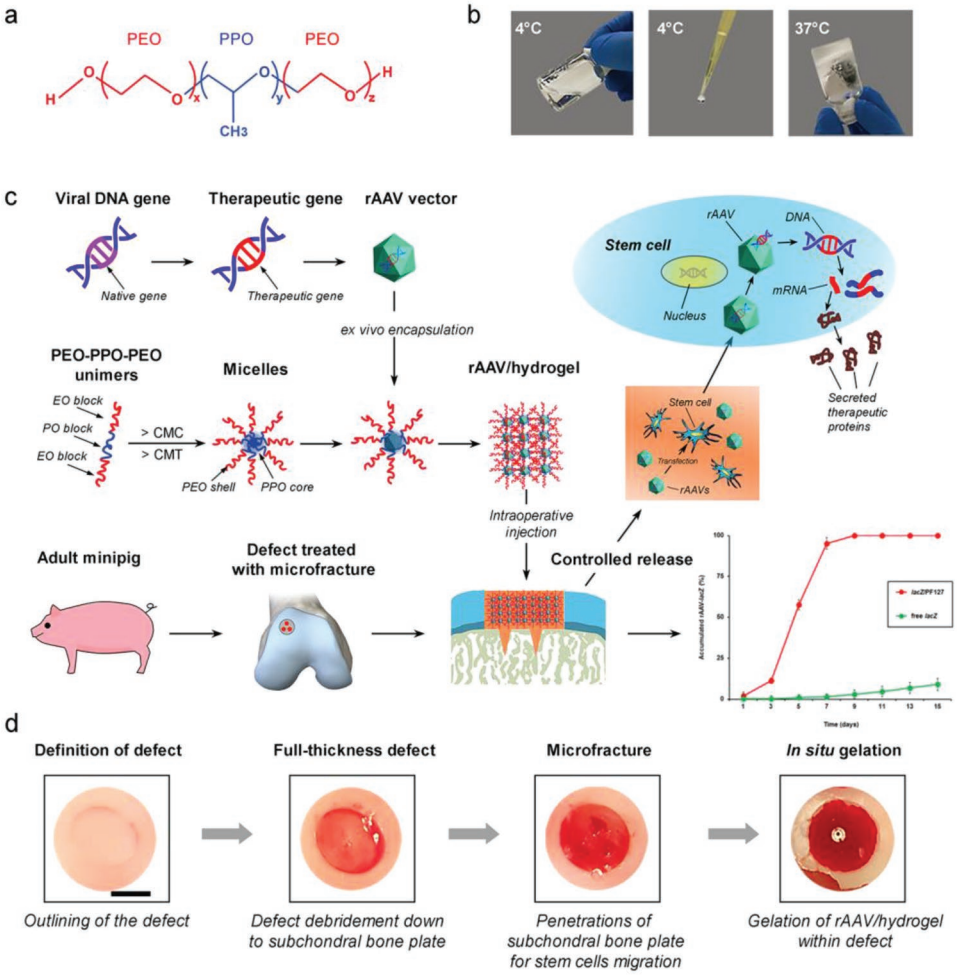

Figure 1. Study design. a) Structure of the PEO–PPO–PEO (PF127) block copolymer. b) Thermosensitive characteristics of the copolymer (liquid form at 4 °C, solid form at 37 °C). c) Flowchart of generation of the rAAV/hydrogel systems for the controlled release of rAAV with implantation in knee full-thickness chondral defects in minipigs following microfracture. The accumulated controlled release pattern of rAAV from PF127 is presented relative to free rAAV. d) Intraoperative view of the full-thickness chondral defect creation and treatment with microfracture augmented with in situ gelation of the rAAV/hydrogels. The defects were outlined in the superior region of the lateral trochlear facets of both knees with a biopsy punch and debrided down to subchondral bone plate after removal of the entire calcified cartilage layer. Three microfracture holes were always introduced per defect in a standardized manner. Then, the PEO–PPO–PEO systems carrying rAAV-FLAG-h*sox9* (*sox9*/hydrogel) or rAAV-*lacZ* (*lacZ*/hydrogel) were directly applied into the treated cartilage defects, allowing for in situ gelation.

the sex-determining region Y-type high-mobility group box 9 transcription factor (SOX9)[9] or the transforming growth factor beta (TGF-β)[10] in human-bone-marrow-derived mesenchymal stromal cells (MSCs)[7] and in human OA chondrocytes or in a human osteochondral defect explant model[8–10] via effective rAAV-vector-controlled release.[8] Of further note, PEO–PPO–PEO copolymer-mediated gene delivery can effectively restore rAAV transduction of MSCs and chondrocytes in inhibitory environments like in the presence of AAV capsid-specific antibodies or of anticoagulants.[8,11] So far, to the best of our knowledge, no study investigated the in vivo efficacy of an injectable hydrogel capable of a controlled in situ release of a therapeutic rAAV vector to improve the repair of cartilage defects in an animal model in vivo. We therefore studied the effects of injecting a thermosensitive hydrogel based on PEO–PPO–PEO poloxamers for the in situ release of an rAAV encoding for the chondrogenic *sox9* transcription factor on the repair of full-thickness chondral defects in a clinically relevant large animal model in vivo.

Adult Göttingen minipigs received standardized full-thickness circular chondral defects in a standardized fashion (diameter = 4.0 mm) in the superior region of the lateral trochlear facet of both stifle joints (Figure 1c) that were each treated with three microfracture holes at identical distances from each other (awl diameter, 1.0 mm) (Figure 1d). In parallel, liquid PEO–PPO–PEO (PF127) hydrogels carrying either the candidate rAAV-FLAG-h*sox9* vector (*sox9*/hydrogel) or a control rAAV-*lacZ* vector (*lacZ*/hydrogel) and showing an effective ability for rAAV controlled release[8] (**Figure 2**d) were injected into the chondral defects, covering the subchondral bone plate and completely filling the defects. In situ gelation of the PEO–PPO–PEO hydrogel always occurred within 2–3 min (Figure 1c). Four weeks postoperatively, the animals were euthanized and the osteochondral units containing the defects were explanted and subjected to standardized macroscopic, histological, immunohistochemical, and micro-computed tomographic (micro-CT) analyses to monitor early osteochondral repair.[12]

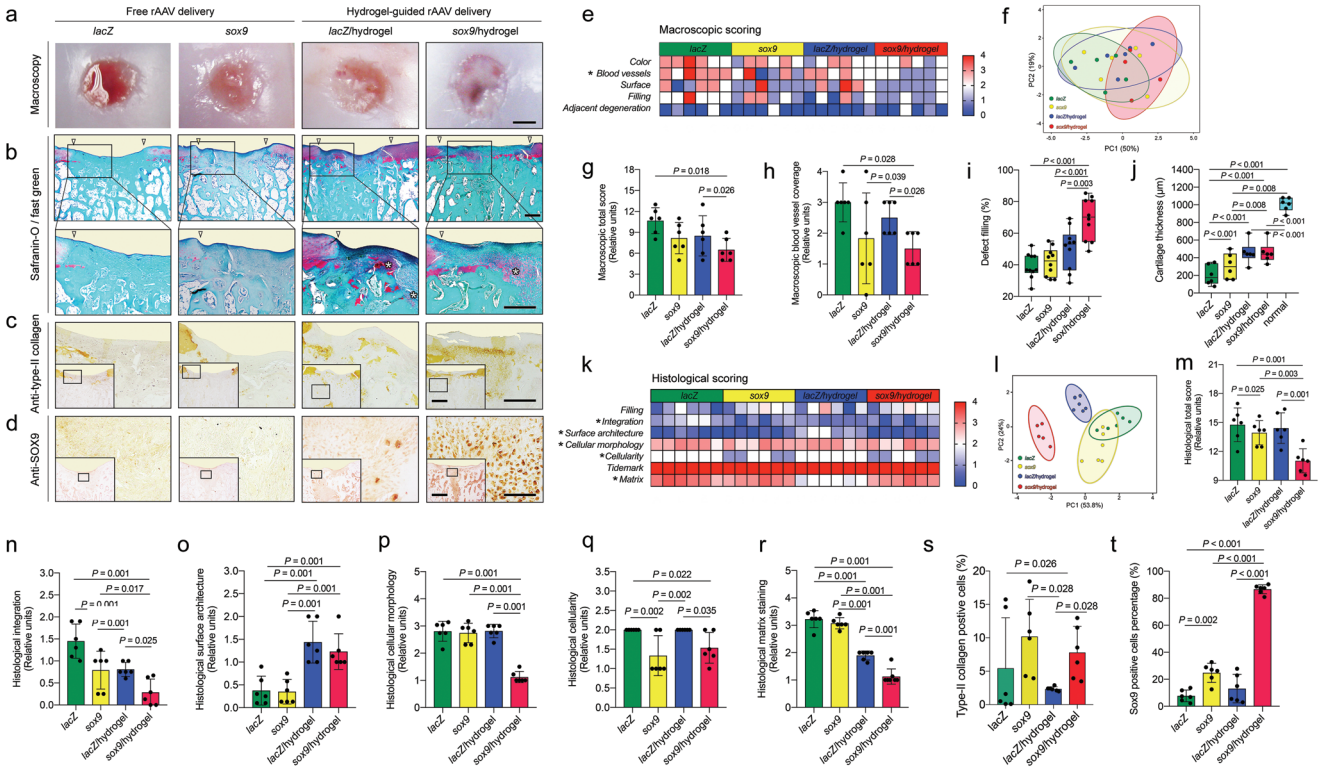

Figure 2. Macroscopic, histological, and immuno-histochemical analyses of cartilage repair in full-thickness chondral defects in minipigs upon microfracture and application of *sox9*/hydrogel versus *lacZ*/hydrogel and free vector treatment 4 weeks postoperatively. a) Macroscopic views (all representative data). b) Histological views showing better repair with larger chondrogenic foci (*) in the *sox9*/hydrogel defects (all representative data). White triangles denote the defect borders. c) Immunodetection of type-II collagen deposition (all representative data). d) Immunodetection of SOX9 expression (all representative data). e) Heat map of variables of the macroscopic scoring with (*) indicating significant intergroup difference for blood vessels coverage. f) Principal component analysis of total macroscopic score underlining the overlapped clusters without clear separations. g) Macroscopic total score. h) Macroscopic blood vessel coverage. i) Defect filling (%). j) Cartilage thickness (µm). k) Heat map of variables of the histological scoring. Variables with significant intergroup differences are shown by (*). l) Principal component analysis of total histological score highlighting the evidently separated clusters of the *sox9*/hydrogel group from all other groups and the overlapping seen between free *sox9* and *lacZ* groups. m) Histological total score. n) Histological integration score. o) Histological surface architecture. p) Histological cellular morphology. q) Histological cellularity. r) Histological matrix staining. s) Type-II collagen-positive cells. t) SOX9-positive cells. Scale bars: a) 2.0 mm, b,c) 0.5 mm, and d) 1.0 mm.

Upon macroscopic evaluation, no joint effusion, inflammation, periarticular osteophyte formation, nor adhesions were observed in any of the treatment groups (Figure 2a). Semiquantitative scoring of macroscopic cartilage repair[13] (Figure 2e,f; Table S1, Supporting Information) revealed significantly improved total scores with the *sox9*/hydrogel ($P = 0.026$ vs *lacZ*/hydrogel, $P = 0.018$ vs *lacZ*) with less new blood vessels covering the repair tissue of defects treated with the *sox9*/hydrogel ($P = 0.026$ vs *lacZ*/hydrogel, $P = 0.028$ vs *lacZ*) (Figure 2g,h; Table S1, Supporting Information). Other individual parameters of the macroscopic scoring were not significantly different between groups ($P \geq 0.093$) (Figure 2e,f; Table S1, Supporting Information).

A histomorphometric analysis revealed that application of the *sox9*/hydrogel significantly improved the filling of the defects relative to all other groups ($P \leq 0.003$) (Figure 2i; Table S2, Supporting Information) while it enhanced the thickness of the cartilage versus free vector treatments ($P \leq 0.008$) although it was significantly thinner than normal cartilage ($P \leq 0.001$) (Figure 2j; Table S2, Supporting Information). A histological analysis (Figure 2b) using a semiquantitative histological scoring of cartilage repair[14] (Figure 2k) further showed that relative to all other groups, application of the *sox9*/hydrogel significantly improved the individual parameters of "integration" ($P \leq 0.025$), "cellular morphology" ($P = 0.001$), and "matrix staining" ($P = 0.001$) (Figure 2n,p,r; Tables S3, Supporting Information) as well as the total histological score of cartilage repair ($P \leq 0.003$) (Figure 2m; Table S3, Supporting Information). The individual parameter of "surface architecture" was improved with the *sox9*/hydrogel versus *lacZ*/hydrogel ($P = 0.001$) while "cellularity" was enhanced versus *lacZ* and *lacZ*/hydrogel ($P \leq 0.022$) (Figure 2o,q; Table S3, Supporting Information). Principal component analysis of the histological scoring (Figure 2l) detected a noteworthy separation among each dataset, indicating significant histological differences of cartilaginous repair tissue between groups. These data extend our previous in vitro findings on the effectiveness of such hydrogel systems as valid delivery platforms for therapeutic rAAV vectors in MSCs, the major cell type responsible for cartilage repair in this in vivo model, as already shown using human MSCs[7] and human articular chondrocytes.[8–10] These data are also in good agreement with the enhanced in vitro chondrogenesis of bone-marrow-derived MSCs[15] and with the improved repair of osteochondral defects in rabbit knee joints by direct, hydrogel-free *sox9* gene transfer.[16]

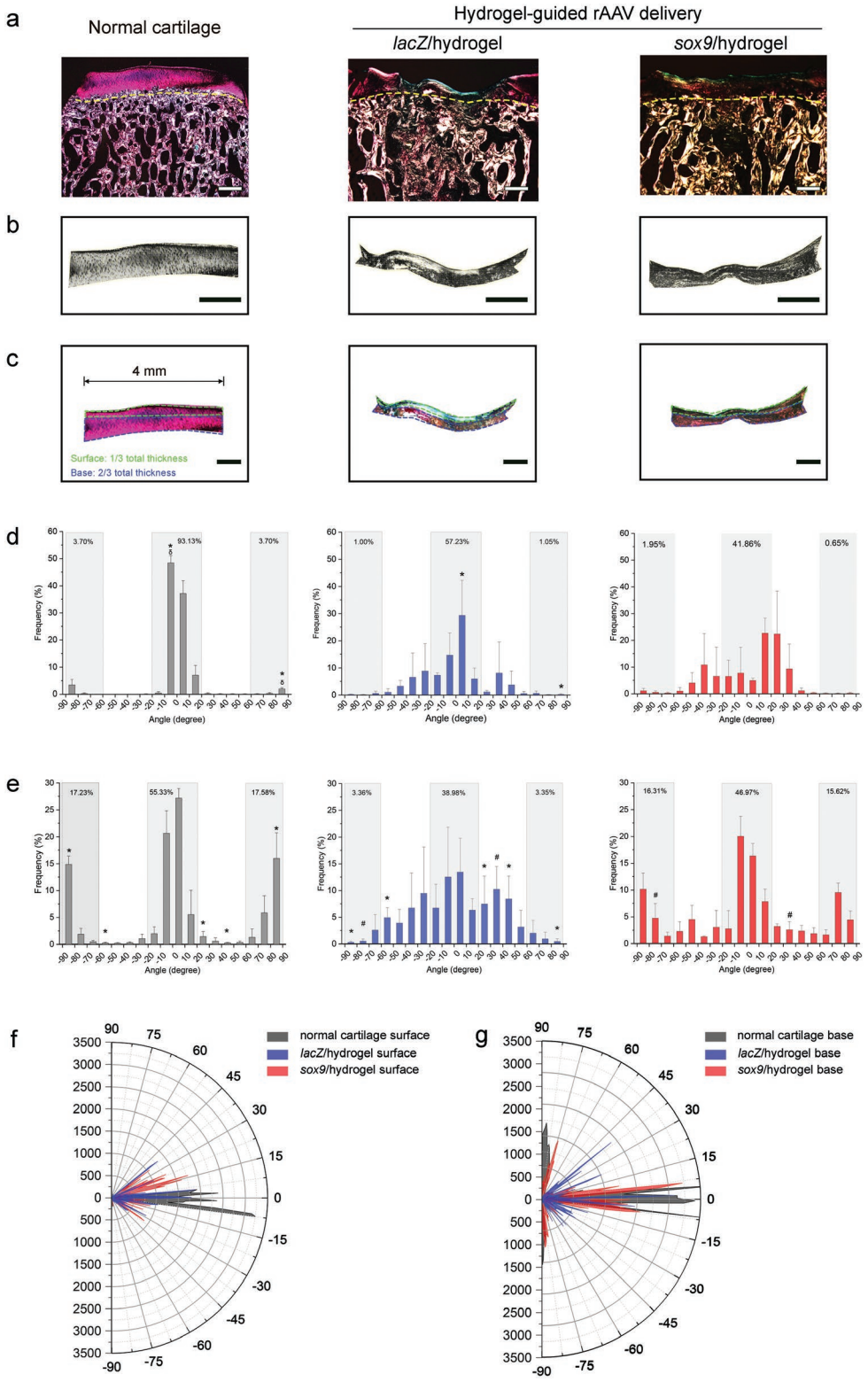

Figure 3. Quantitative analyses of collagen fiber orientation of the repair tissue within the articular cartilage zone. a) Representative polarized microscopic views of normal cartilage and defects from both treatment groups. b) Vector filed illustration. c) Region of interests (ROIs) within the articular cartilage zone: surface ROI with one-third total thickness and base ROI with two-thirds total thickness. d) Collagen orientation within the surface ROI. e) Collagen orientation within the base ROI. $^{*}P \leq 0.05$ for comparison between normal cartilage and *lacZ*/hydrogel defects; $^{\delta}P \leq 0.05$ for comparison between normal cartilage and *sox9*/hydrogel defects; $^{\#}P \leq 0.05$ for comparison between both groups. f,g) Radar charts of collagen orientation within both surface (f) and base (g) ROIs.

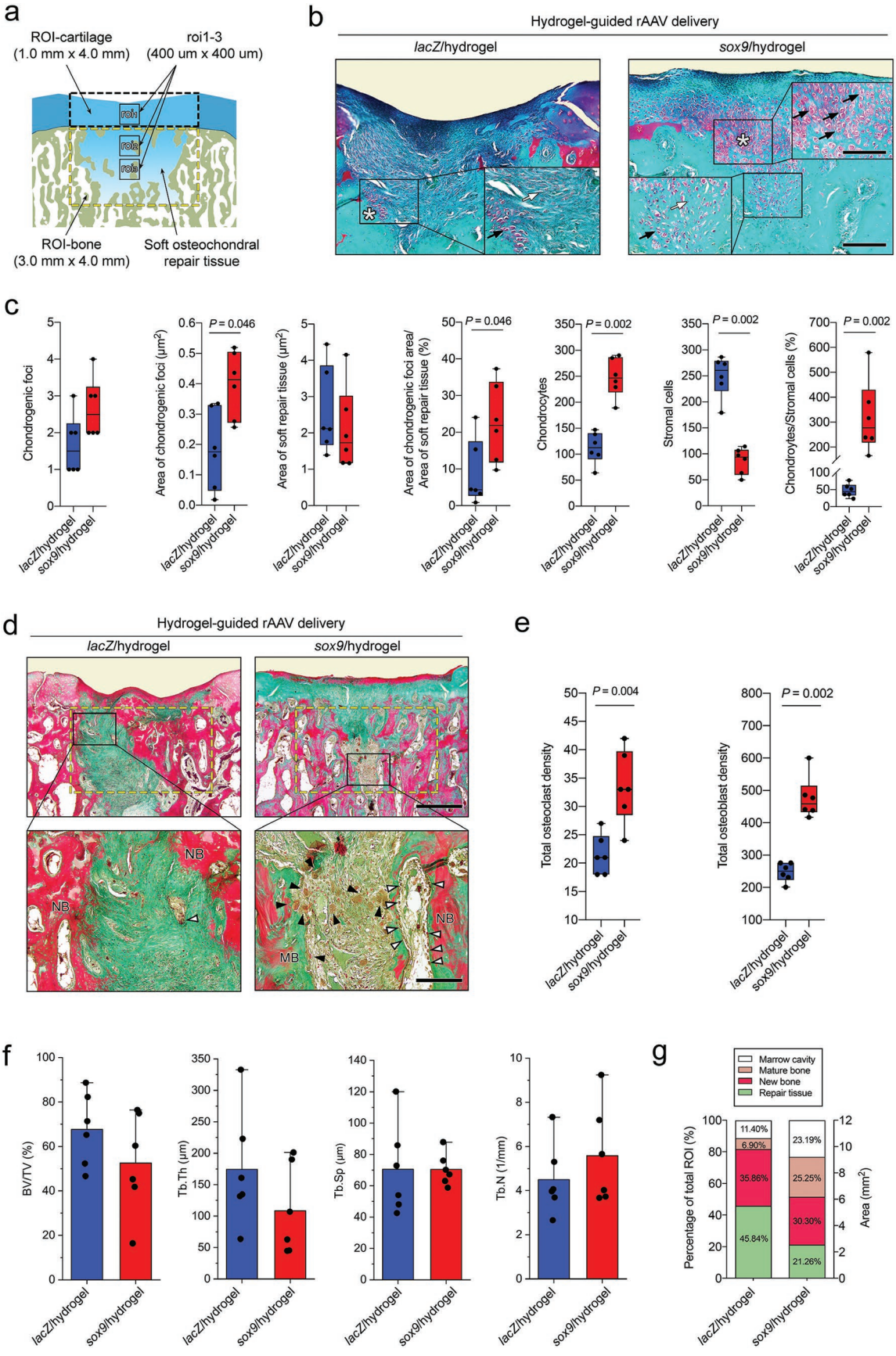

We also observed higher type-II collagen deposition in the *sox9*/hydrogel defects compared with the *lacZ*/hydrogel group or with free *lacZ* application ($P \leq 0.026$) (Figure 2c,s; Table S4, Supporting Information), probably resulting from higher numbers of SOX9-positive cells in the *sox9*/hydrogel defects relative to all other groups ($P \leq 0.001$) (Figure 2d,t; Table S4, Supporting Information), indicating improved transgene expression via PEO–PPO–PEO-guided rAAV controlled release.

An immuno-histochemical analysis on histological sections to detect potential CD3 (T-lymphocytes), CD11b (activated macrophages), and human leukocyte antigen isotype DR alpha (HLA-DRα) (class II major histocompatibility complex (MHC) antigens) expression[17] revealed the quasiabsence of immune cells in all the defects without significant differences between groups ($P \geq 0.220$) (Figure S1 and Table S5, Supporting Information). The absence of immune response in the current design, even after long time body exposure to the vectors, is in good agreement with our previous findings in vivo using rAAV vectors in a free form[16] and with the observation that PEO–PPO–PEO poloxamers can protect rAAV-mediated gene transfer from neutralization by antibodies directed against the AAV capsid in vitro and in experimental cartilage defects.[8,11] Overall, these observations further confirm the benefits of applying this class of gene vehicles for clinical purposes compared with the effective but highly immunogenic and transient adenoviral vectors.[18]

As such evaluations overall demonstrated superior cartilage repair via hydrogel-guided rAAV delivery over free rAAV vector treatment, we next focused on in-depth microstructural, comparative analyses in the *sox9*/hydrogel versus *lacZ*/hydrogel groups. An evaluation of collagen orientation and distribution detected visually better and more collagens distributed in positive degree toward the subchondral bone plate in the basal zone of the *sox9*/hydrogel defects than in the *lacZ*/hydrogel defects (Figure S2, Supporting Information). Further analyses revealed differences between groups in two subregions of interest (ROIs) of the cartilaginous repair tissue (**Figure 3**a–c). Compared with the surface zone of normal cartilage, significant less collagens oriented between −10° and 0° and between 80° and 90° were observed in either group compared with normal cartilage (Figure 3d,f). Within the basal zone of the cartilaginous repair tissue, collagen orientation in the *lacZ*/hydrogel defects showed significant different patterns in multiple degree ranges (from −90° to −80°, −60° to −50°, 20° to 30°, 40° to 50°, and 80° to 90°; all $P \leq 0.05$) compared with normal cartilage, while the *sox9*/hydrogel defects showed orientation and distribution of collagens more analogous to normal cartilage (Figure 3e,g). These findings suggest that *sox9*/hydrogel delivery yielded a better approximation of the normal zonal collagen network than the control condition, especially in the basal zone. Mimicking the primary vertical orientation in the base zone of the normal cartilage, these restored collagen fibrils by *sox9* treatment may significantly increase the stiffness of the tissue and protect the solid matrix against large distortions and strains at the subchondral junction,[19] possibly yielding a persistent and enhanced cartilaginous repair tissue.

We next performed histomorphometric analyses to determine the effects of the rAAV/hydrogels on chondrogenesis and osteogenesis within the osteochondral unit in vivo (**Figure 4**a,b). Compared with the *lacZ*/hydrogel defects, the *sox9*/hydrogel defects exhibited a significantly larger area of mature chondrogenic foci ($P = 0.046$) with a significantly improved area of chondrogenic foci/soft repair tissue ratio ($P = 0.046$) (Figure 4c; Table S6, Supporting Information). Moreover, significantly more chondrocytes, less MSCs, and higher cellularity ratio of chondrocytes versus MSCs were observed in the osteochondral repair tissue of the *sox9*/hydrogel defects compared with the control defects ($P = 0.002$). Taken together, these data indicate that *sox9* treatment via PEO–PPO–PEO hydrogel-guided delivery significantly improved major parameters of a stratified zonal in situ chondrogenesis.[20]

As microfracture also exerts effects on the subchondral bone,[21] we also searched for possible subchondral bone changes in the defects (Figure S3, Supporting Information). Histomorphometric analyses evidence newly formed bone always located at the margin of the soft repair tissue. Application of the *sox9*/hydrogel led to a significantly higher total osteoclast ($P = 0.004$) and osteoblast ($P = 0.002$) density in the repair tissue and marrow cavity than the control group (Figure 4d,e). 2D bony structure parameters (bone volume fraction, BV/TV; trabecular thickness, Tb.Th; trabecular separation, and Tb.Sp; trabecular number, Tb.N) and measurements of structural components (marrow cavity, mature and new bone, and repair tissue) were not significantly different ($P \geq 0.05$) (Figure 4f,g; Table S7, Supporting Information).

Applying a micro-CT-based algorithm,[22] residual microfracture holes, perihole bone resorption, and intralesional osteophytes (*lacZ*/hydrogel: $n = 2$; *sox9*/hydrogel: $n = 1$) were identified in both groups without significant differences ($P \geq 0.05$) (Figure S3, Supporting Information). An analysis of all 18 microfracture holes per group showed no significant differences in the perihole bone resorption and bone bridge

Figure 4. Histomorphometric analyses of chondrogenesis and osteogenesis in the osteochondral unit. a) Illustration of the regions of interest (ROIs). ROIs of osteochondral unit include both articular cartilage (ROI-cartilage; black dashed rectangle) and subchondral bone (ROI-bone; yellow dashed rectangle). Quantification of chondrogenic foci was performed within both ROI-cartilage and ROI-bone, while quantification of chondrocytes and bone-marrow-derived MSCs was achieved within the center of the osteochondral unit within up to three additional defined ROIs (roi1-3; black rectangles), depending on the depth of the soft osteochondral repair tissue. b) Representative chondrogenic foci (white *) with chondrocytes (black arrows) and MSCs (white arrows). Note the more mature and larger chondrogenic foci in the *sox9*/hydrogel defects than in the *lacZ*/hydrogel defects. c) Significantly larger area of chondrogenic foci and area ratio of chondrogenic foci to soft repair tissue with considerably more chondrocytes, less MSCs, and higher cellularity ratio of chondrocytes to MSCs in the osteochondral repair tissue in the *sox9*/hydrogel defects than the *lacZ*/hydrogel defects. The numbers of chondrogenic foci and area of soft repair tissue are comparable between both groups. d) Bone histomorphometry within ROI-bone. Note the interference of newly formed bone (NB) within the mature bone (MB) at the margin of soft repair tissue and osteoblasts (white arrowheads) and osteoclasts (black arrowheads) within the repair tissue and marrow cavity. e) Significantly higher total osteoclast and osteoblast density within the repair tissue of the *sox9*/hydrogel defects than the *lacZ*/hydrogel defects. f) No differences in BV/TV, TB.Th, Tb.Sp, and Tb.N between both groups. g) Percentage of areas occupied by marrow cavity (white), mature bone (light red), new bone (red), and soft repair tissue (green) within ROI-bone of both groups.

height between groups ($P \geq 0.05$) (Tables S8 and S9, Supporting Information). Microstructural evaluation of the entire region below the cartilage defect revealed a considerable early affection of the subchondral bone plate in both groups, with decreased BV/TV, specific bone surface (BS/BV), bone surface density (BS/TV), and cortical thickness (Ct.Th) compared with the normal osteochondral unit (Figure S4, Supporting Information). Such early loss of the subchondral bone induced by microfracture suggests that stimulation of new bone formation underlying the treated defects possibly occurs at later time points[23] and, from a clinical perspective, highlights the importance of a protected weight bearing within the first 6 weeks postoperatively when performing marrow stimulation in the tibiofemoral compartment.[24] Of special importance, *sox9*/hydrogel treatment led to a significantly higher BV/TV of the subchondral bone plate than the control treatment ($P = 0.002$), suggesting a preserving effect of the *sox9*/hydrogel on the subchondral bone plate. The subarticular spongiosa was less affected by such changes, as no differences of BV/TV, BS/BV, and Tb.Th were found between the normal osteochondral unit and defects treated by either the *lacZ*/hydrogel or the *sox9*/hydrogel ($P \geq 0.05$). Treatment with the *lacZ*/hydrogel yielded significantly less BS/TV than the normal osteochondral unit ($P = 0.002$) (Table S10, Supporting Information).

This study holds some limitations. First, the 4 week time point selected for assessment of early osteochondral repair does not allow for a final assessment of the long-term effectiveness. Second, the full postoperative weight bearing as requested by animal welfare is not comparable to a clinical rehabilitation. The strengths of the study include the use of a translational animal model at an early time point, allowing for an in-depth analysis of the very early outcomes of marrow stimulation, and the comprehensive analyses of the entire osteochondral unit based on a variety of robust evaluation methods using categorical and continuous data.

Taken together, the present study shows, for the first time to our best knowledge, that a thermosensitive hydrogel based on PEO–PPO–PEO poloxamers controlling the release of a therapeutic (*sox9*) rAAV vector significantly improves the repair of full-thickness chondral defects in a clinically relevant large animal model in vivo. These copolymers are highly promising materials for in vivo rAAV delivery, supporting cartilage repair in conditions where protection against potentially damaging host immune responses may need to be afforded. The data support the concept of advanced biomaterial-guided delivery of gene carriers as an attractive therapeutic option for cartilage repair, enabling for a controlled and minimally invasive delivery[25] of genes without loss of the therapeutic gene product in vivo. From a clinical translational point of view, such biomaterial-guided gene vector delivery is particularly attractive for cartilage defects that are arthroscopically treated with microfracture and may represent a major step toward improved cartilage repair in the near future.

Supporting Information

Supporting Information is available from the Wiley Online Library or from the author.

Acknowledgements

H.M. and L.G. contributed equally to this work. This project was supported by the Deutsche Forschungsgemeinschaft (DFG RE 3828/2-1). All animal experiments were conducted in agreement with the national legislation on protection of animals and the National Institutes of Health (NIH) Guidelines for the Care and Use of Laboratory Animals (NIH Publication 85-23, Rev 1985) and were approved by the Saarland University Animal Committee according to German guidelines.

Conflict of Interest

The authors declare no conflict of interest.

Keywords

biomaterial-guided therapy, cartilage defects, gene therapy, rAAV, tissue engineering

Received: October 4, 2019
Published online: November 25, 2019

[1] A. Guermazi, D. Hayashi, F. W. Roemer, J. Niu, E. K. Quinn, M. D. Crema, M. C. Nevitt, J. Torner, C. E. Lewis, D. T. Felson, *Arthritis Rheumatol.* **2017**, *69*, 560.
[2] J. M. Hootman, C. G. Helmick, *Arthritis Rheum.* **2006**, *54*, 226.
[3] T. D. Brown, R. C. Johnston, C. L. Saltzman, J. L. Marsh, J. A. Buckwalter, *J. Orthop. Trauma* **2006**, *20*, 739.
[4] M. Cucchiarini, H. Madry, *Nat. Rev. Rheumatol.* **2019**, *15*, 18.
[5] C. Alvarez-Lorenzo, A. Rey-Rico, A. Sosnik, P. Taboada, A. Concheiro, *Front. Biosci.* **2010**, *E2*, 424.
[6] K. T. Oh, T. K. Bronich, A. V. Kabanov, *J. Controlled Release* **2004**, *94*, 411.
[7] P. Diaz-Rodriguez, A. Rey-Rico, H. Madry, M. Landin, M. Cucchiarini, *Int. J. Pharm.* **2015**, *496*, 614.
[8] A. Rey-Rico, J. Frisch, J. K. Venkatesan, G. Schmitt, I. Rial-Hermida, P. Taboada, A. Concheiro, H. Madry, C. Alvarez-Lorenzo, M. Cucchiarini, *ACS Appl. Mater. Interfaces* **2016**, *8*, 20600.
[9] A. Rey-Rico, J. K. Venkatesan, G. Schmitt, S. Speicher-Mentges, H. Madry, M. Cucchiarini, *Mol. Pharmaceutics* **2018**, *15*, 2816.
[10] A. Rey-Rico, J. K. Venkatesan, G. Schmitt, A. Concheiro, H. Madry, C. Alvarez-Lorenzo, M. Cucchiarini, *Int. J. Nanomed.* **2017**, *12*, 6985.
[11] A. Rey-Rico, J. K. Venkatesan, J. Frisch, I. Rial-Hermida, G. Schmitt, A. Concheiro, H. Madry, C. Alvarez-Lorenzo, M. Cucchiarini, *Acta Biomater.* **2015**, *27*, 42.
[12] P. Orth, C. Peifer, L. Goebel, M. Cucchiarini, H. Madry, *Prog. Histochem. Cytochem.* **2015**, *50*, 19.
[13] L. Goebel, P. Orth, A. Muller, D. Zurakowski, A. Bucker, M. Cucchiarini, D. Pape, H. Madry, *Osteoarthritis Cartilage* **2012**, *20*, 1046.
[14] L. A. Fortier, H. O. Mohammed, G. Lust, A. J. Nixon, *J. Bone Jt. Surg., Br. Vol.* **2002**, *84-B*, 276.
[15] K. Tao, J. Frisch, A. Rey-Rico, J. K. Venkatesan, G. Schmitt, H. Madry, J. Lin, M. Cucchiarini, *Stem Cell Res. Ther.* **2016**, *7*, 20.
[16] M. Cucchiarini, P. Orth, H. Madry, *J. Mol. Med.* **2013**, *91*, 625.
[17] S. A. Rodeo, A. Seneviratne, K. Suzuki, K. Felker, T. L. Wickiewicz, R. F. Warren, *J. Bone Jt. Surg., Am. Vol.* **2000**, *82*, 1071.
[18] a) C. H. Evans, S. C. Ghivizzani, T. A. Oligino, P. D. Robbins, *Arthritis Res.* **2001**, *3*, 142; b) D. Bellavia, F. Veronesi, V. Carina,

V. Costa, L. Raimondi, A. De Luca, R. Alessandro, M. Fini, G. Giavaresi, *Cell. Mol. Life Sci.* **2018**, *75*, 649.
[19] Q. Meng, S. An, R. A. Damion, Z. Jin, R. Wilcox, J. Fisher, A. Jones, *J. Mech. Behav. Biomed. Mater.* **2017**, *65*, 439.
[20] A. Chevrier, C. D. Hoemann, J. Sun, M. D. Buschmann, *Osteoarthritis Cartilage* **2011**, *19*, 136.
[21] P. Orth, H. Madry, *Tissue Eng., Part B* **2015**, *21*, 504.
[22] L. Gao, P. Orth, L. K. Goebel, M. Cucchiarini, H. Madry, *Sci. Rep.* **2016**, *6*, 32982.
[23] L. Gao, P. Orth, K. Muller-Brandt, L. K. Goebel, M. Cucchiarini, H. Madry, *Sci. Rep.* **2017**, *7*, 45189.
[24] a) J. R. Steadman, W. G. Rodkey, J. J. Rodrigo, *Clin. Orthop. Relat. Res.* **2001**, *391*, S362; b) H. Madry, L. Gao, H. Eichler, P. Orth, M. Cucchiarini, *Stem Cells Int.* **2017**, *2017*, 1609685.
[25] N. Ashammakhi, S. Ahadian, M. A. Darabi, M. El Tahchi, J. Lee, K. Suthiwanich, A. Sheikhi, M. R. Dokmeci, R. Oklu, A. Khademhosseini, *Adv. Mater.* **2019**, *31*, 1804041.